Influence of carbon content on microstructure and properties of a steel matrix cermet

P. Alvaredo, P. Bruna, D. Crespo, E. Gordo

PII: S0263-4368(18)30134-3
DOI: doi:10.1016/j.ijrmhm.2018.04.006
Reference: RMHM 4707

To appear in: *International Journal of Refractory Metals and Hard Materials*

Received date: 27 February 2018
Revised date: 2 April 2018
Accepted date: 8 April 2018

Please cite this article as: P. Alvaredo, P. Bruna, D. Crespo, E. Gordo , Influence of carbon content on microstructure and properties of a steel matrix cermet. The address for the corresponding author was captured as affiliation for all authors. Please check if appropriate. Rmhm(2018), doi:10.1016/j.ijrmhm.2018.04.006

Influence of carbon content on microstructure and properties of a steel matrix cermet

P. Alvaredo[a]*, P. Bruna[b], D. Crespo[b], E. Gordo[a]

[a]Departamento Ciencia e Ingeniería de Materiales. Universidad Carlos III Madrid.

Avda. de la Universidad, 30, 28911 Leganés (Spain)

[b]Departamento Física Aplicada, EETAC, Universitat Politècnica Catalunya.

Esteve Terradas 5, 08860 Castelldefels (Spain)

**Corresponding author*: palvared@ing.uc3m.es Tel: +34 91 624 9482 Fax: +34 91 624 9430

Abstract

There is a marked correlation between the composition, microstructure and properties in TiCN-based cermets. In the case of using iron alloys as metallic matrix the carbon content is of particular significance, as not only influences the stoichiometry of ceramic phase but also induces phase transformations in the steel matrix. However, such influence has been less studied in steel matrix cermets than in conventional Ni or Co ones, so the aim of this work is to contribute to the study of the influence of carbon content on the microstructure and properties of a steel matrix cermet containing fixed quantities of alloying elements. Samples were prepared by powder metallurgy and characterized combining different techniques as Transmission Mössbauer spectroscopy (TMS), X Ray diffraction (XRD), field emission scanning electron microscopy (FE-SEM) and transmission electron microscopy (TEM), to explain differences found in hardness and toughness.
Keywords: TiCN, Fe Cermets, Transmission Mössbauer spectroscopy, X-ray diffraction, and transmission electron microscopy

1. Introduction

TiCN-based cermets are metal-ceramic composite materials in which the metallic matrix is mainly Ni and/or Co, although in the last years small amount of other metals as Al and Fe are used. Moreover, carbides of transition elements as WC, Mo_2C, TaC, NbC… are added to the ceramic phase to adjust the properties to the requirements [1, 2]. Namely, a wide range of compositions might be used in this type of composite materials and there is an intense relationship between their composition, microstructure and properties.

The presence of transition elements allows the formation of a solid solution (Ti, M)(C, N) (M: W, Mo, Ta, Nb…) around the TiCN particles resulting in the typical core-rim microstructure of TiCN-based cermets. The formation of this microstructure has been widely studied and it is accepted that the mechanism of formation implies the partial dissolution of TiCN particles during liquid phase sintering and subsequent reprecipitation enriched in transition elements during cooling [3, 4] and not a decomposition of TiCN [5] or diffusion of the transition elements to TiCN particles [6].

The presence of the solid solution (Ti, M)(C, N) (Rim) around TiCN particles (Core) allows: a) to improve the wettability between the metallic matrix and ceramic reinforcement during the liquid phase sintering; b) a better dispersion of the reinforcement particles and c) to avoid the coarsening of ceramic particles. Consequently, finer and more homogeneous microstructures are obtained which are reflected in an increase of hardness and toughness. However, the improvement of toughness only occurs when the rim has a thickness less than 0.5 μm because with a higher thickness the toughness decreases abruptly because tensions are created between the core and the rim which cause the initiation and crack propagation during service [7-9].

Another factor to take into account in the design of the composition of these cermets is the carbon content. Several studies analyzed the influence of carbon content on the microstructure and properties of TiCN-based cermets. The main conclusions that can be drawn from them are: 1) C favors the dissolution of heavy metals in the metallic matrix [10], and 2) C promotes the dissolution-precipitation mechanism of the TiCN particles during the sintering, namely, the formation of the solid solution (Ti, M)(C,N) [11, 12]. However these studies are focused in Co/Ni matrix cermets and few studies have been found in steel matrix cermets [13, 14]. These studies agree on the great influence of carbon content in the microstructure of the cermet, and hence the final properties.

The use of an iron alloy as metallic matrix provides some advantages in relation to the use of the conventional metallic matrix, Ni and Co, as lower price and toxicity and the ability to be hardened by heat treatment. In fact, due to its advantages iron is used as metallic matrix in TiC-based cermets [15]. Moreover, the iron alloy can be selected to contain the alloying elements required to design the microstructure, in a similar way than the addition of secondary carbides of transition elements in Co/Ni based cermets. In this the metallic matrix used is a high speed steel, M2 grade with Mo and W in its composition. The presence of these alloying elements not only increase the

amount of hard phase in the cermet because they are carbides formers, but also improves the wetting behavior during the liquid phase sintering of the compound material [16].
Although in general it is important to know the influence of C content in cermets, in the case of steel matrix cermets the C content has further significance. Besides the influence on the composition and distribution of TiCN particles, carbon is needed for the formation of carbides of alloying elements, and can also change the phases present in the steel matrix. All these characteristics lead to different properties of the material and it is important to understand the influences. In this work, a characterization study is shown to find out the influence of C content on the microstructure and properties of a steel matrix cermet containing W, Mo, V and Cr as alloying elements.

2. Experimental procedure

The investigated composite material consists of a steel metallic matrix and 50 vol.% of $Ti(C_{0.5},N_{0.5})$ particles as a reinforcement phase. The composition of the steel is 6.2 wt.% W, 4.8 wt. Mo, 4.1 wt.% Cr, 1.8 wt.% V and 0.85 wt.% C, which corresponds to the high-speed steel grade M2, used as prealloyed powder. To study the effect of the carbon content, different amounts of graphite were added to the matrix leading to materials with composition [M2 + X wt.% C] + TiCN 50 vol.%, where X is 0, 0.5 and 1. The density and particle size of the starting powders are given in Table 1.

Table 1. Characteristics of raw materials.

The powders were blended for 4 hours in a Turbula® multidirectional mixer, and then processed by the conventional powder metallurgy route (CPS): uniaxial pressing at 700 MPa into rectangular bars (31 mm x 13 mm x 4 mm) and sintering in vacuum (10^{-4} mbar) at 1400 ºC for 60 minutes, the heating and cooling rates of the sintering cycle were 5 ºC/min. Hardness was measured in Vickers scale with 30 kg load (HV30) and the fracture toughness was measured by three point bending test of notched samples with dimensions 28 mm x 3.6 mm x 3.2 mm. The notch was performed with a femtopulsed laser beam, to ensure regular dimensions of the notch, especially the radius at the bottom. The density measurement was performed by He picnometer.
The carbon present in the sintered samples was measured by chemical analysis performed by LECO equipment. The microstructural characterization was performed by: X-Ray Diffraction (XRD) analysis in Philips X´Pert equipment, Scanning Electron Microscopy (SEM) in Philips XL-30 equipment and Field Emission Scanning Electron Microscopy (FEG-SEM) in Nova NanoSEM230 coupled with an electron Dispersive X-ray (EDX) EDAX SUTW Zafiro Si(Li).
The steel matrix phases were characterized by room temperature Transmission Mössbauer spectroscopy (TMS) [17]. The spectra were obtained using a conventional constant acceleration

spectrometer and using a 25 mCi source of ^{57}Co in Rh matrix. The spectra were recorded in 512 channels of a multichannel analyzer using a maximum velocity of 2.47 mm/s and 10.00 mm/s. Experimental spectra were fitted with Brand´s NORMOS program [18]. The isomer shift values (δ) are relative to room temperature Fe-α. All the samples have been fitted using four sub-spectra: three sextets and one singlet. Low velocity spectra were fitted using one doublet, one or two singlets and one or two sextets.

With the purpose of studying the hard phase of the cermet and avoid the interactions of the metallic matrix, the hard phase was isolated by removing the metallic matrix. The samples were introduced during 4 hours in an acid solution (HNO_3/HCl 1:3) which dissolved the steel matrix. The powder obtained after the dissolution was characterized by Transmission Electron Microscopy (TEM, Jeol Jem 2000FX).

3. Results

The microstructures of the steel matrix cermet, M2/Ti(C,N), with different C content are shown in Figure 1. The three materials show the same three phases on the microstructure: the steel matrix (grey), the TiCN particles (black) and a third bright phase corresponding with the carbides of the alloy elements from the high speed steel matrix. Although at first sight these microstructures are quite similar, there are some important differences: (1) the morphology and distribution of the carbides of the alloying elements is different in the cermet without C addition, as these carbides are placed in the steel matrix whereas in the cermet with 0.5 and 1.0 wt. % of C the carbides are placed surrounding the TiCN particles. (2), the microstructure of the cermets with C addition seems to be more homogeneous than the microstructure of the cermet without C addition which shows zones in the steel matrix free of reinforcement.

It is not possible by SEM to distinguish other phases in the steel matrix or significant changes in the composition of carbides and carbonitrides. However, the properties measured, density, hardness and fracture toughness, present a clear relationship with the C content, as shown in Figure 2. It is shown that the hardness and toughness of the samples with 0.5 and 1.0 wt. % of C, which present full density, are much higher than hardness and toughness of the sample with no C addition which shows a relative density of 96.4 %. Then it makes necessary a deeper study of the material, for which a combination of techniques was used.

Figure 1. SEM microstructures of the sintered cermet M2/Ti(C,N) with different C content: 0; 0.5 and 1.0 wt. %.

Figure 2. Hardness and fracture toughness of the sintered samples of M2/Ti(C,N) as a function of the C added to the steel matrix.

To study the phases formed in the M2/Ti(C,N) with different C content (0; 0.5 and 1.0 wt. % C), XRD analysis of the sintered samples were performed and the resultant XRD diffractograms are presented in Figure 3. In the three cases the peaks corresponding to the main phases can be observed: i) the peaks corresponding with TiCN reinforcement, ii) the peaks corresponding with the steel matrix, and iii) the peaks corresponding to the carbides of the alloying elements from the high speed steel matrix. The main differences found between the diffractograms are related to the steel phases: by increasing the carbon content the relative intensity of the main peak of ferrite decreases and a peak of austenite appears. These changes may be due to the steel phase changes with the carbon addition.

However it is not possible to extract more information from these analyses as this technique presents two limitations: i) the steel phases, martensite and ferrite, are difficult to distinguish due to their similar pattern diffraction; ii) the characterization of the carbides of the alloying elements from high speed steel is difficult due to the complexity of their composition and the lack of reference patterns for all the possible combinations.

To characterize the steel phases present in the cermet with different C content and to characterize the carbides of the alloy elements complementary techniques to XRD have been used.

Figure 3. XRD analysis of [M2 + x wt. %. C]/ Ti(C,N) (x = 0; 0.5; 1.0) sintered samples.

3.1 Characterization of the steel matrix

In order to characterize the steel phases present in the cermet M2/Ti(C,N) with different C content (0; 0.5 and 1.0 wt. %) Mössbauer spectroscopy was used to analyze the samples. The three spectra obtained after Transmission Mössbauer Spectroscopy (TMS) analyses are shown in Figure 4 where the growth of a paramagnetic phase (central peak) upon the C addition is clearly seen. This paramagnetic phase is fitted with one singlet with an isomer shift value (δ) of ~ -0.1 mm/s characteristic of an austenitic phase [19]. The remaining ferromagnetic phase can be fitted with three sextets with hyperfine magnetic field values (B) close to 33.5, 31.0 and 28.0 T and isomer shift values of -0.01, -0.02 and -0.05 mm/s, respectively. These values are typical of ferrite/martensite subspectra [20]. In Table 2 is shown a complete report of the hyperfine parameters for all the samples.

Figure 4. Transmission Mössbauer Spectroscopy (TMS) spectra for the cermet (M2/Ti(C,N) with different C content 0; 0.5 and 1.0 wt. %)

Table 2. Mössbauer hyperfine parameters and sub-spectral areas for the cermet M2/Ti(C,N) with different C content (0; 0.5; 1.0 wt. %): isomer shift values (δ), quadrupole splitting (Δ), Full width at half maximum

(FWHM) of the peaks (Γ), hyperfine magnetic field (B) and relative area of each sub-spectra. (Statistical errors are given in parentheses. No error means that the parameter was fixed in the fitting)

From Figure 4 it is also clear that the contribution of the ferromagnetic phase decreases with the C content up to the addition of 0.5 wt. %, when the amount of each phase remains almost constant. This can be seen clearly in Figure 5 where the atomic percentage of each phase as determined from the area of each Mössbauer spectra is represented. Although the total amount of ferromagnetic and paramagnetic phases remains constant for C contents higher than 0.5 wt. %, the contributions of the three sextets of the ferromagnetic phase keep varying as it can be observed in Figure 5.

The paramagnetic subspectra are related to a face centered cubic (FCC) crystal structure; in this case, austenite (Fe-γ), while the ferromagnetic sub-spectra corresponds with a body centered cubic (BCC) crystal structure. In this later case, the spectra can be related either to ferrite (Fe-α) or martensite but the Mössbauer parameters for each of these phases are the same, making it impossible to distinguish between them when there are other elements that can be introduced in the structure as interstitial or substitutional. The reason is twofold: on the one hand, the effect of non-magnetic substitutional atoms in the structure of ferrite is to induce a reduction in B seen by the Fe atom resulting in B values around 33, 31 and 29 T for 8, 7 and 6 nearest neighbours, respectively. On the other hand, martensite has some interstitial C atoms that results in three main environs as seen by the Fe atom in a non-substituted martensite: Fe atoms with no C atoms neighbours with a B of 33 T, Fe atoms with co-planar C neighbour with a B of 30.5 T and Fe atoms closest to a C neighbour with a B of 27.5 T [21]. Being the isomer shift and quadrupole splitting values identical in both structures is very difficult to distinguish ferrite from martensite using only Mössbauer spectrometry. Moreover, although theoretically being able to distinguish subspectra with so close values of B like 31 and 30.5 T or 29 and 27.5 T, it will be impossible to distinguish between non-substituted ferrite and martensite with no C neighbours. However, with this in mind and assuming that the addition of C does not change the amount of substitutional atoms in the structure, some conclusions can be drawn from Figure 5. The clear effect of adding C is to favour the austenite phase (from nearly 2 at. % to 10 at. %), this implies that the interstitial C can be distributed in this phase instead of being in the ferrite/martensite phase. This is clearly seen in the increase of percentage of Fe atoms with a B of 33 T and the decrease of the Fe atoms with lower field values (Figure 5a). Figure 5a also shows that the ferromagnetic component with a B of 31 T remains almost constant for C amounts higher than 0.5 wt. %. Taking into account the above assumption, it can be said that the Fe environs in martensite with co-planar C neighbours are stable upon the C addition.

Figure 5. a) Atomic percentage of Fe in each sextet of the ferromagnetic phase as a function of C content. b) Atomic percentage of Fe in ferromagnetic and paramagnetic phases as a function of C content.

More information on the C content on the austenite phase can be obtained by taking the Mössbauer spectra at a low source velocity in order to get a better accuracy in the central part of the spectra. Therefore, low velocity spectra of the samples with 0, 0.5 and 1 wt. % C addition were obtained and can be seen in Figure 6. The paramagnetic component can be fitted with three subspectra corresponding to: (i) Fe atoms without near-neighbor or next-near C atoms that results in a singlet, (ii) Fe atoms with only one near-neighbor C atom, yielding a doublet, and (iii) Fe atoms without near-neighbor C atoms but with n next-near neighbor atoms, resulting in another singlet [22]. In particular, the hyperfine parameters of Fe atoms in type (ii) environments are clearly distinguishable in the studied spectra and from the area of this subspectrum the atomic percentage of Fe atoms in this environment can be determined.

The ratio between Fe atoms in type (ii) environments and interstitial C atoms is 6:1 [23]. This allows us to determine the concentration of C atoms in the austenite phase as: $cC=A_{ii}/6$ where A_{ii} is the relative area of the doublet corresponding to Fe atoms in type (ii) environments. It should be noted that for the 0 wt. % C case, a second doublet had to be added in the fitting procedure in order to obtain good results. This second doublet has not been identified yet but it could be attributed to some residual Fe-Cr phase. In any case, this doublet does not affect the fitting of the austenitic doublet, thus allows us to calculate the C content in the austenite phase with accuracy. Table 3 shows the total atomic C concentration in the sintered samples as well as the atomic C concentration in austenite, computed as explained above. The difference between these two concentrations is the remaining C in the ferrite and martensite phases. As it is impossible to distinguish between ferrite with some substitutional C and martensite, we can only calculate the maximum C concentration in martensite, which would correspond to having only C-free ferrite. Accordingly, the maximum concentration of martensite is computed assuming that the Fe:C ratio in this phase is 14:1 (see also Table 3).

Figure 6. Transmission Mössbauer Spectroscopy (TMS) spectra at low velocity (±2.47 mm/s) for the cermet M2/Ti(C,N) with different C content (0; 0.5; 1.0 wt. %).

Table 3. Atomic percentages of C in the different phases and the maximum amount of martensite.

3.2 Hard phase characterization

To characterize the hard phase of the composite material, that is, Ti(C,N) particles reinforcement and the carbides of the alloying elements from the steel matrix, FE-SEM and TEM have been used. The microstructures observed by FE-SEM are shown in Figure 7.

Figure 7. FE-SEM microstructures of the sintered cermet M2/Ti(C,N) with 0; 0.5 and 1.0 wt. % C. EDS analysis of the black core and the brighter rim in Ti(C,N) reinforcement particles

Regarding to the Ti(C,N) particles it is observed that in the cermet with 0.5 and 1.0 wt. % C a brighter rim appears around Ti(C,N) particles resembling the typical core/rim structure of Ti(C,N)-based cermets. The results of the EDS analysis of the black core and the brighter rim in Ti(C,N) reinforcement particles are also indicated in Figure 7. The analysis of the black core only shows the presence of Ti, C and N; while the analysis of the brighter rim also shows the presence of W and Mo, which could indicate the formation of the (Ti, W, Mo)(C,N) solid solution as occurs in cermets with conventional Ni and Co metallic matrixes [24].

Besides, differences in the morphology and situation of carbides of alloying elements from the steel are also observed in the microstructures shown in Figure 7. The microstructure of the cermet with no C addition shows only one type of carbide with a rounded morphology and a composition rich in W and Mo, whereas in cermets with 0.5 and 1.0 wt % C there are two types of carbides: Type I, with rounded morphology and a composition rich in Mo; and Type II, with a needle shape and a composition rich in V.

For a further characterization of these carbides, samples of M2/Ti(C,N) with 0.5 wt. %C were subjected to an etching processing to dissolve the metallic matrix and isolate the carbides in order to be analyzed by Transmission Electron Microscopy (TEM). In Figure 8 TEM images and diffraction patterns of the two carbides found are shown. The microanalysis of the rounded carbide (Type I) indicates that the composition of this carbide is (at.%): 46.4 V; 20.5 Ti; 19.8 Mo; 8.0 W; 5.2 Cr, and the diffraction pattern indicates that the structure of this carbide is face centered cubic (FCC) with Fm3m symmetry. Comparing with the typical carbides found on high speed steels the carbide Type I could be a MC type carbide which present FCC structure and is V-rich.

Figure 8. TEM image and pattern diffraction of the Type I and Type II carbides of the cermet M2/Ti(C,N) with 0.5 wt. % C.

The microanalysis of the needle-shape carbide (Type II) indicates that the composition of this carbide is (at. %): 34.3 Mo; 24.2 W; 16.1 V; 13.1 Cr; 12.2 Ti. The diffraction pattern indicates that the structure of this carbide is hexagonal compact with P63/mmc symmetry. Comparing with the typical carbides found on high speed steels the Type II carbide could be M_2C type carbide which is the only type of carbides presenting this HCP structure, and is Mo-rich.

4. Discussion.

By increasing the C content the melting temperature of the steel matrix decreases, as it can be observed in the phase diagram of the cermet M2 HSS/TiCN showed in the reference [25], so that

the cermet without C added presents a higher melting temperature and the dissolution-reprecipitation mechanism is not completed, while in the cermet with 0.5 and 1.0 wt. % C the melting temperature is lower and the sintering mechanism can be completed resulting in a different microstructure, leading to higher hardness and toughness.

The differences of the microstructure by increasing the C content are found in both the steel matrix and hard phase. The changes produced in the steel matrix are related to the steel phases present. Table 4 summarizes the amount of steel phases present in the sintered samples with different C additions obtained from Mössbauer spectra. It is observed a decrease in ferrite quantity by increasing the C content. The maximum percentage of austenite is observed in the sample with 0.5 wt. % and the sample with 1.0 wt. % shows high martensite percentage.

Table 4. Steel phases amount in sintered samples of M2/Ti(C,N) with different C addition (0; 0.5; 1.0 wt. %)

By increasing the C content to 0.5 and 1.0 wt. % it is also observed that the TiCN particles show a microstructure similar to the typical core/rim microstructure of TiCN-based cermets. The presence of the solid solution (Ti, M)(C, N) rim around the TiCN particles is claimed to improve the wettability between the metallic matrix and reinforcement particles and, also, inhibits their growth and avoids their agglomeration during the processing [7, 9] in conventional cermets. As a similar structure is observed, it can be assumed that it could also be responsible of the same benefits in the case of this steel matrix, as properties of cermets improves significantly and, what is more interesting, hardness and toughness increase simultaneously.

Another reason for the improvement of hardness with increasing the C content is the presence of the MC type and M_2C type carbides, which are the hardest types of carbides which could be found in high speed steels. However M_2C type carbides are not the typical carbides found on high speed steel M2 grade which are MC and M_6C. The absence of M_6C carbides and the presence of M_2C may be due to the nature of this material. This is a metal matrix composite which is a high speed steel with a high percentage (50 vol. %) of TiCN as ceramic reinforcement. The presence of these particles can have an impact on the formation of carbides in the steel matrix. In this microstructure the alloying elements W and Mo are forming a solid solution in TiCN. In this new material the presence of the rim around the particles of TiCN was observed which can be responsible for the different stoichiometry of the carbides formed in the matrix. It is possible that the formation of the solid solution (Ti, M) (C, N) causes a reduction in the alloying elements amount of the matrix and, therefore, the formation of carbides with a lower ratio metal / carbon.

5. Conclusions.

The hardness and fracture toughness of the steel-matrix cermet studied, M2/50Ti(C,N), show a significant increment with C content. As a result of the characterization study presented in this work, this improvement is attributed to the microstructural changes observed when C content of the steel matrix is at least 0.5 wt. %, and which it can be summarized as follows:

- Appearance of austenite and increase of martensite in the steel matrix.

- Presence of the solid solution (Ti,M)(C,N) around the TiCN particles resembling the typical core/rim microstructure of conventional TiCN-based cermets. M is Mo or W.
- Formation of MC type and M_2C type carbides which are the hardest carbides in high speed steels.

6. Acknowledgements.

The authors would like to acknowledge the financial support from the Spanish Government through the project MAT2015-70780-C4-1-P and MAT2015-70780-C4-2-P, the Regional Government of Madrid through the program MULTIMAT-CHALLENGE, ref. S2013/MIT-2862, and Generalitat de Catalunya for Grants Nº 2009SGR1225 and Nº 2009SGR1251. The fracture toughness values were obtained thanks to the technical support and equipment of Prof. Pastor, from UPM.

References.

[1] W. Wan, J. Xiong, Y. Li, Q. Tang, M. Liang. Erosion-corrosion behavior of Ti(C,N)-based cermets containing different secondary carbides. Int. J. Refract. Met. Hard Mater. 66 (2017) 180-187.

[2] W. Wan, J. Xiong, M. Liang. Effects of secondary carbides on the microstructure, mechanical properties and erosive wear of Ti(C,N)-based cermets. Ceram. Int. 43 (2017) 944-952.

[3] H. Suzuki H., Terada O., Mechanisms of surrounding structure formation in sintered TiC–Mo2C–Ni alloys, Journal of japanese institute of metallurgy 35 (1981) 245-273.

[4] H.-O. Andrén, Microstructure development during sintering and heat-treatment of cemented carbides and cermets, Mat. Chem. Phys., 67 (2001) 209-213.

[5] E. Rudy, Constitution of ternary Titanium-Tungsten-Carbon alloys, Journal of the Less-Common Metals, 33 (1973) 245-273.

[6] H.M. Moskowitz D, Cemented titanium carbide cutting tools, Modern developments in powder metallurgy, 3 (1966).

[7] H. Zhang, J. Yan, X. Zhang, S. Tang, Properties of titanium carbonitride matrix cermets, Int. J. Refract. Met. Hard Mater, 24 (2006) 236-239.

[8] J. Jung, S. Kang, Effect of ultra-fine powders on the microstructure of Ti(CN)–xWC–Ni cermets, Acta Mater., 52 (2004) 1379-1386.

[9] T. Laoui, H. Zou, O. Van der Biest, Analytical electron microscopy of the core/rim structure in titanium carbonitride cermets, Int. J. Refract. Met. Hard Mater, 11 (1992) 207-212.

[10] N. Liu, X. Liu, X. Zhang, L. Zhu, Effect of carbon content on the microstructure and mechanical properties of superfine Ti(C, N)-based cermets, Mater. Charac., 59 (2008) 1440-1446.

[11] Y. Li, N. Liu, X. Zhang, C. Rong, Effect of carbon content on the microstructure and mechanical properties of ultra-fine grade (Ti,W) (C,N)-Co cermets, J. Mater. Process. Tech., 206 (2008) 365-373.

[12] J. Zackrisson, H.O. Andrén, Effect of carbon content on the microstructure and mechanical properties of (Ti, W, Ta, Mo)(C, N)-(Co, Ni) cermets, Int. J. Refract. Met. Hard Mater, 17 (1999) 265-273.

[13] H. Yu, W. Liu, Y. Zheng, Effect of carbon content on the microstructure and mechanical properties of Mo2FeB2 based cermets, Int. J. Refract. Met. Hard Mater, 29 (2011) 724-728.

[14] P. Alvaredo, S.A. Tsipas, E. Gordo, Influence of carbon content on the sinterability of an FeCr matrix cermet reinforced with TiCN, Int. J. Refract. Met. Hard Mater, 36 (2013) 283-288.

[15] C.S.M. A. Evans, A. Mortensen, Metal Matrix Composites in Industry: An Introduction and a Survey, in, Springer, 2003.

[16] P. Alvaredo, J.J. Roa, E. Jiménez-Pique, L. Llanes, E. Gordo. Characterization of interfaces between TiCN and iron-base binders. Int. J. Refract. Met. Hard Mater, 63 (2017) 32-37

[17] R. Giovanelli, A. Orefice, Physical discussion of the Mössbauer effect, Physica B., 293 (2000) 155-163.

[18] L.L. Brand R., Herlach D., The evaluation of hyperfine field distributions in overlapping and asymmetric Mossbauer spectra: a study of the amorphous alloy Pd77.5-xCu6Si16.5Fex, J. Phys. F: Met. Phys., 13 (1984) 675-668.

[19] D. Oleszak, A. Grabias, M. Pękała, A. Świderska-Środa, T. Kulik, Evolution of structure in austenitic steel powders during ball milling and subsequent sintering, J. Alloys Compds, 434–435 (2007) 340-343.

[20] D.J. Laneri K.F., Mercader R.C., Gregorutti R.W., Sarutti J. L., Thermal dependence of austempering transformation kinetics of compacted graphite cast iron, Metall. Mater. Trans. A, 32A (2001) 51-58.

[21] K.A. Ron M., Schechter H. , Niedzwiedz S. , Structure of Martensite, J. Appl. Phys., 38 (1967) 590-594.

[22] P.T. Bruna P. , Crespo D. , García-Mateo C. , Bhadeshia K. K. D. H. , Mössbauer analysis of low temperature bainite, in: J.F.M. Mercedes Gracia, Fernando Plazaola (Ed.) AIP Conference, 2005, pp. 338-343.

[23] B.J.P. Uwakweh O. N. C. , Génin J.-M. R. , Mössbauer study of the distribution of carbon interstitiels in iron alloys and the isochronal kinetics of the aging of martensite: The clustering-ordering synergy, Metall. Mater. Trans. A, 21 (1990) 589-602.

[24] A. Demoly, W. Lengauer, C. Veitsch, K. Rabitsch, Effect of submicron Ti(C,N) on the microstructure and the mechanical properties of Ti(C,N)-based cermets, Int. J. Refract. Met. Hard Mater, 29 (2011) 716-723.

[25] P. Alvaredo, D. Mari, E. Gordo, High temperature transformations in a steel-TiCN cermet, Int. J. Refract. Met. Hard Mater, 41 (2013) 115-120.

Table 1. Characteristics of raw materials.

Raw material	Supplier	Supplier data		Experimental data	
		Density (g/cm^3)	Particle size (µm)	Density (g/cm^3)	Particle size (µm)
$Ti(C_{0.}5,N0_{.5})$	H.C. Starck	5.03	D50 = 2.0 - 4.0	5.12	D50 = 3.9 D90 = 8.6
High Speed Steel, M2	Osprey	8.56	D90<16	8.09	D50= 8.1 D90 = 15.8

Table 2. Mössbauer hyperfine parameters and sub-spectral areas for the cermet M2/Ti(C,N) with different C content (0; 0.5; 1.0 wt. %): isomer shift values (δ), quadrupole splitting (Δ), FWHM of the peaks (Γ), hyperfine magnetic field (B) and relative area of each sub-spectra. (Statistical errors are given in parentheses. No error means that the parameter was fixed in the fitting)

Sample	Sub-spectrum	δ (mm/s)	Δ (mm/s)	Γ (mm/s)	B (T)	Area (%)	Area (%)
0%C	Sextet 1	-0.08(2)	0.042(4)	0.326(9)	33.95(2)	31.7(1)	98.2(2)
	Sextet 2	0.018(2)	0.040(4)	0.41(1)	31.03(2)	39.8(1)	
	Sextet 3	0.043(5)	0.06(1)	0.53(2)	28.19(6)	26.7(1)	
	Singlet	-0.1	-	0.52(6)	-	1.8(1)	1.8(1)
0.5%C	Sextet 1	-0.013(4)	0.034(9)	0.35(2)	33.91(4)	34.01(1)	70.8(2)
	Sextet 2	-0.03(1)	0.05(2)	0.44(5)	31.3(1)	21.0(1)	
	Sextet 3	-0.072(1)	0.07(5)	0.5(1)	28.9(2)	15.79(1)	
	Singlet	-0.101(4)	-	0.53(6)	-	29.2(1)	29.2(1)
1.0%C	Sextet 1	-0.017(4)	0.025(8)	0.34(1)	33.45(3)	50.1(1)	76.2(2)
	Sextet 2	-0.020(9)	0.05(2)	0.30(4)	30.87(8)	19.8(1)	
	Sextet 3	-0.090	0.07	0.5(2)	28.2	6.3(1)	
	Singlet	-0.1	-	0.58(2)	-	23.8(1)	23.8(1)

Table 3. Atomic percentages of C in the different phases and the maximum amount of martensite.

C added (wt. %)	0	0.5	1.0
C Total (at. %)	2.86	4.57	6.97
C Austenite (at. %)	0.08 (5)	1.8 (4)	3.1 (5)
Max C in martensite (at. %)	2.78(5)	2.7 (4)	3.87 (5)
Max martensite (at. %)	39 (1)	38 (5)	54 (7)

Table 4. Steel phases amount in sintered samples of M2/Ti(C,N) with different C addition (0; 0.5; 1.0 wt. %)

(M2 + X%C)/TiCN	X = 0.0	X = 0.5	X = 1.0
Martensite (at. %)	39	38	54
Ferrite (at. %)	59.2	32.8	22.6
Austenite (at. %)	1.8	29.2	23.8

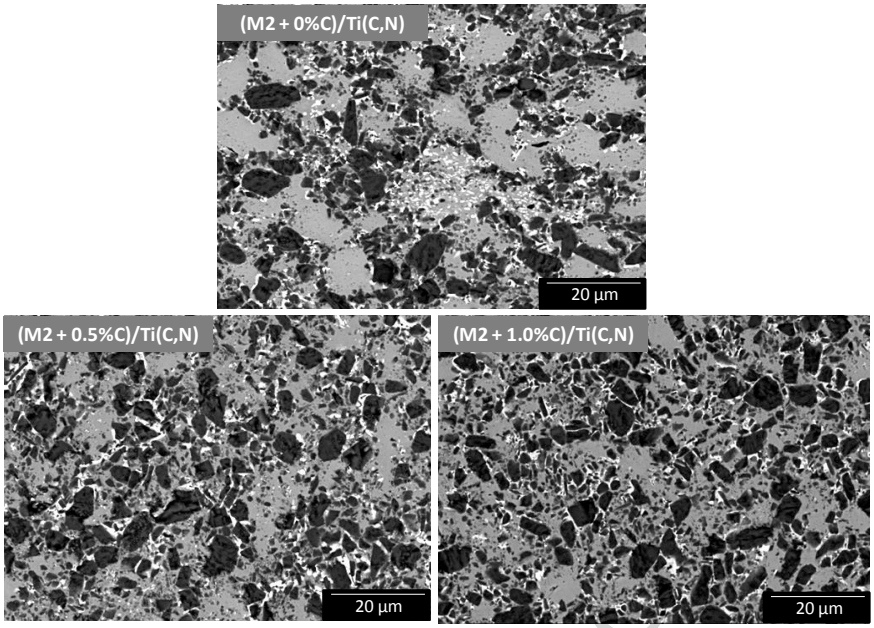

Figure 1. SEM microstructures of the sintered cermet M2/Ti(C,N) with different C content: 0; 0.5 and 1.0 wt. %.

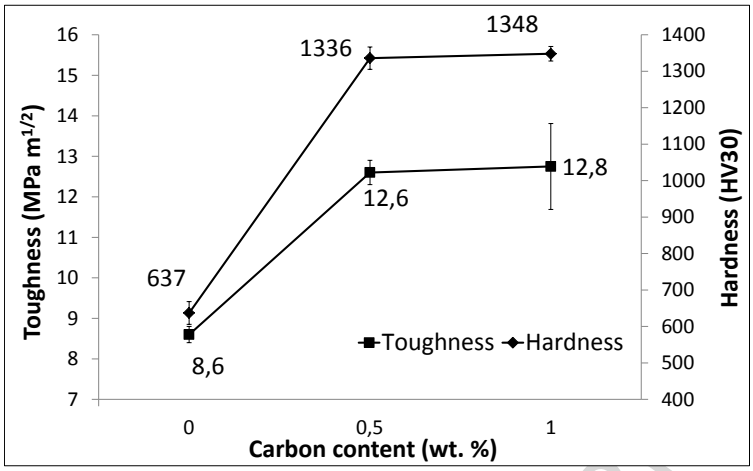

Figure 2. Hardness and fracture toughness of the sintered samples of M2/Ti(C,N) as a function of the C added to the steel matrix.

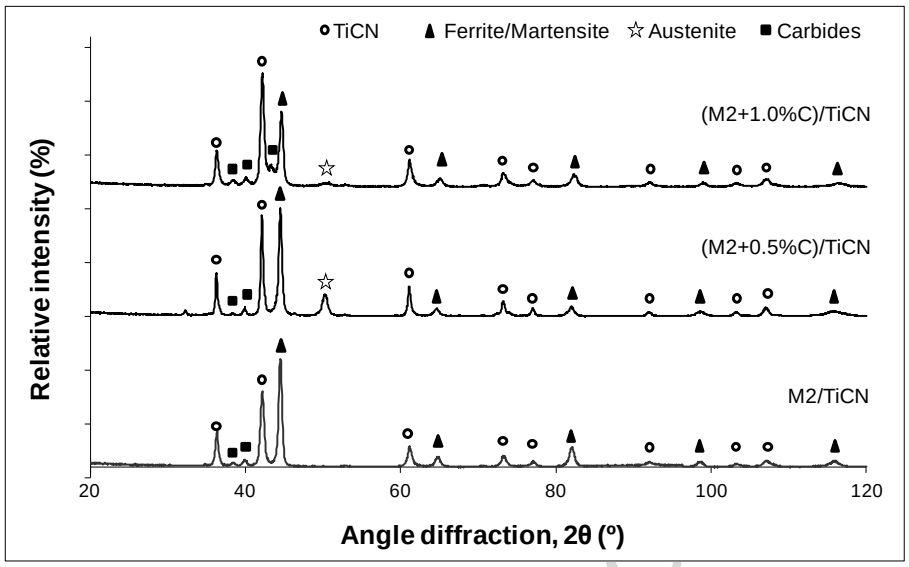

Figure 3. XRD analysis of [M2 + x wt. %. C]/ Ti(C,N) (x = 0; 0.5; 1.0) sintered samples.

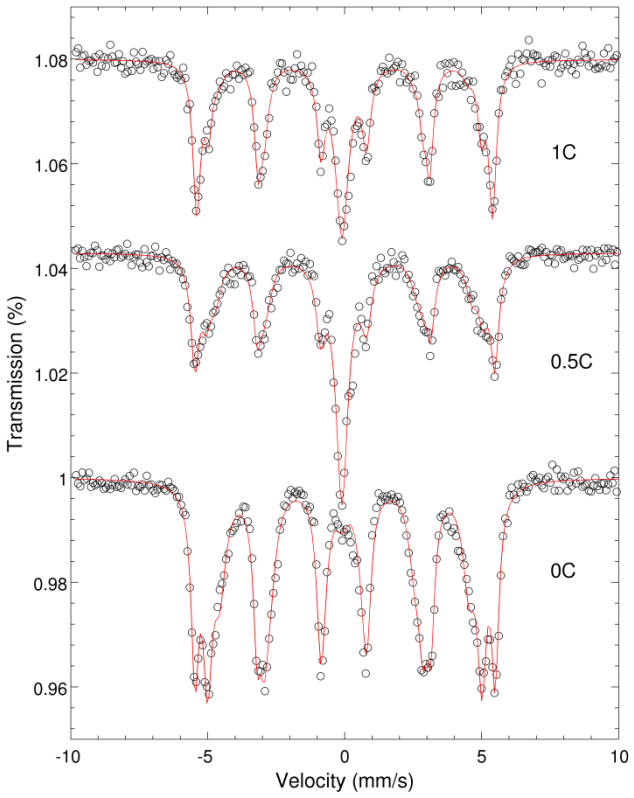

Figure 4. Transmission Mössbauer Spectroscopy (TMS) spectra for the cermet (M2/Ti(C,N) with different C content 0; 0.5 and 1.0 wt. %)

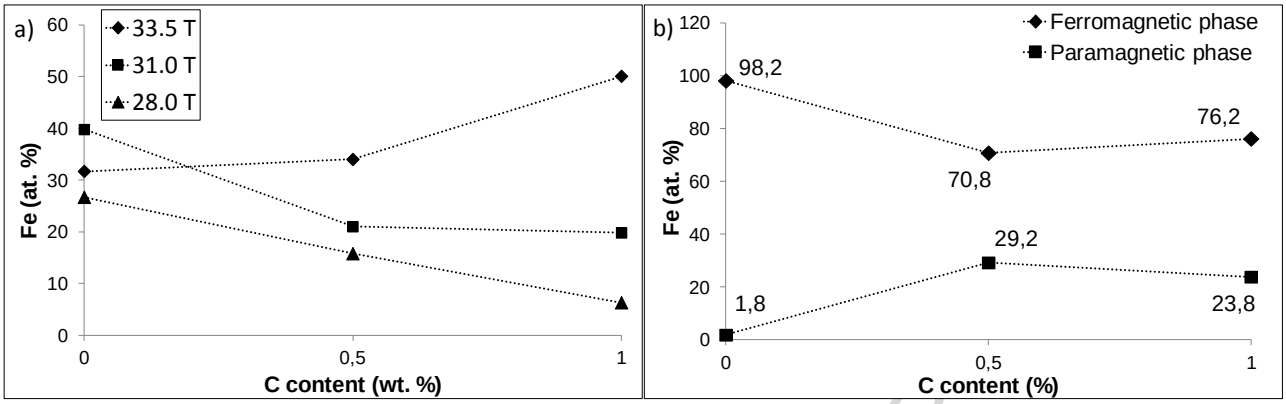

Figure 5. a) Atomic percentage of Fe in each sextet of the ferromagnetic phase as a function of C content. b) Atomic percentage of Fe in ferromagnetic and paramagnetic phases as a function of C content.

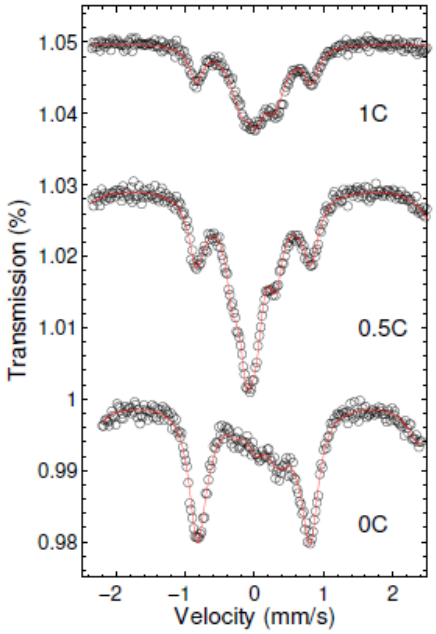

Figure 6. Transmission Mössbauer Spectroscopy (TMS) spectra at low velocity (± 2.47 mm/s) for the cermet M2/Ti(C,N) with different C content (0; 0.5; 1.0 wt. %).

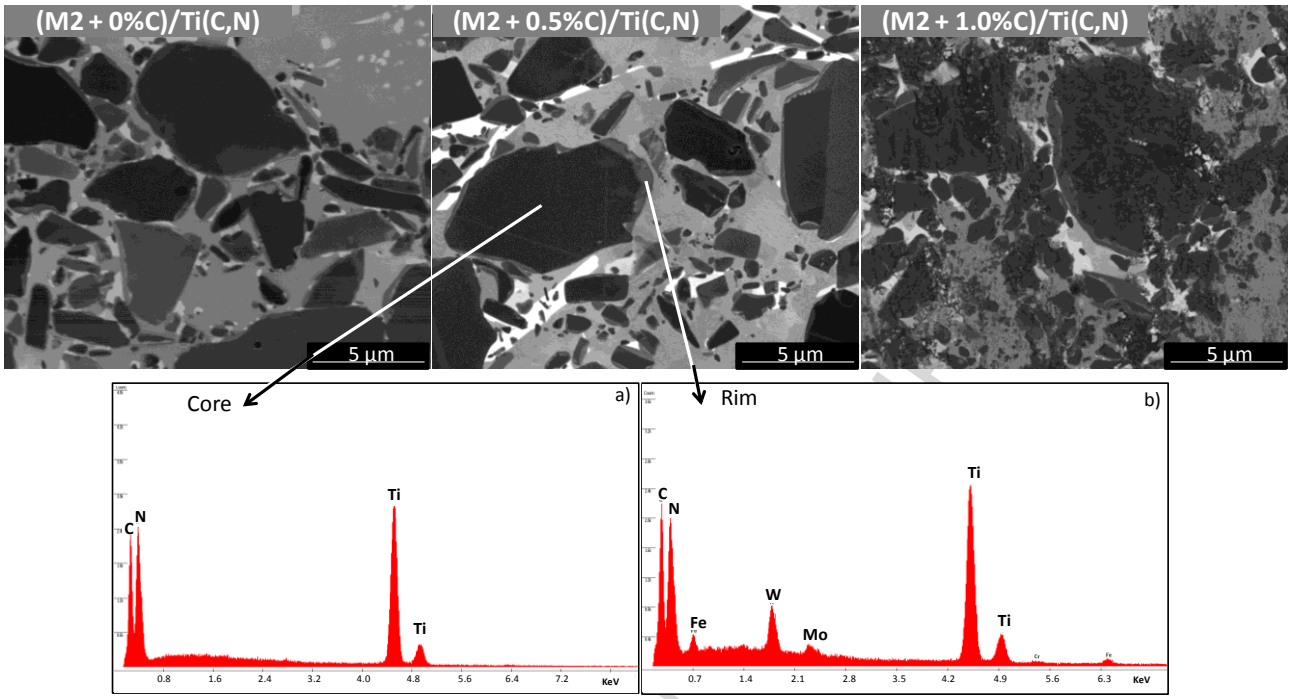

Figure7. FE-SEM microstructures of the sintered cermet M2/Ti(C,N) with 0; 0.5 and 1.0 wt. % C. EDS analysis of the black core and the brighter rim in Ti(C,N) reinforcement particles

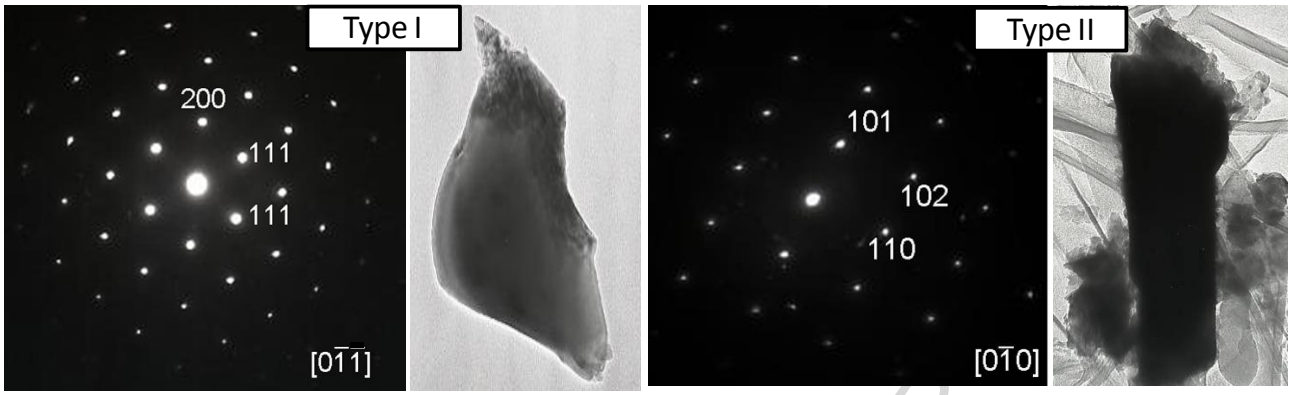

Figure 8. TEM image and pattern diffraction of the Type I and Type II carbides of the cermet M2/Ti(C,N) with 0.5 wt. % C.

Highlights

- Large increase in hardness and toughness by increasing carbon content.
- Appearance of austenite and increase of martensite by increasing carbon content.
- Presence of solid solution (Ti,M)(C,N) resembling the typical core-rim structure